Supplementary Data

Supplementary Methods

Western blot methodology

Differentially expressed proteins [lung-derived mesenchymal stromal cells (L-MSCs) vs. bone marrow-derived mesenchymal stromal cells (BM-MSCs)] were further corroborated using immunoblots. Cells were lysed in ice cold buffer (T-Per, Tissue Protein Extraction Reagent; Pierce) with protease inhibitors added (Roche Complete Mini Protease Inhibitor Tab with ethylenediaminetetraacetic acid; Roche). Protein concentrations were measured using BCA assay (Thermo-Scientific/Pierce). The cell lysate was further prepared in Laemmli sample buffer with 2-mercaptoethanol added (5%), and heated to 95°C. The resulting sample (30 μg/sample) was loaded into each well of a 1MM 4%–20% Tris-glycine gel (Criterion Gel; BioRad) and separation was performed at 100–120 V for 90 min. Proteins were transferred onto polyvinylidene fluoride (PVDF) blotting paper at 2°C–4°C. Efficiency of transfer was confirmed by both Ponceau S red staining (PVDF membrane) and Coomassie blue (sodium dodecyl sulfate-gel). After blocking PVDF membrane for 1–2 h at 21°C with 4% casein, samples were incubated with primary antibodies (intercellular adhesion molecule 1 [ICAM-1], platelet derived growth factor receptor alpha [PDGFRα], or Itg α2, 1:500–1,000) overnight (4°C). Detection was performed using peroxidase-linked secondary antibodies (Vector Laboratories, Elite ABC kit; product # PK-6101) and a diaminobenzidene (DAB) reporter system (Vector laboratories; product # SK-4100). All samples/PVDF were reprobed for beta-actin antibody (1:20,000 dilution) as a protein loading control for normalization of signals.

Quantitative real-time PCR methodology

Lung tissue RNA was isolated by flooding the lung intratracheally with RNAlater solution (Qiagen #76104), followed by storage of lung tissue samples in RNAlater at −80°C. Total RNA was isolated using a combination of TRIzol reagent (Invitrogen), and the Purelink RNA mini kit (Invitrogen) according to the manufacturer's directions. Total RNA concentrations, A260/A280 ratios, and RNA integrity number (RIN) values were determined using an Agilent 2100 Bioanalyzer (Agilent Technologies). Cultured L-MSCs or BM-MSCs (0.5×10^6) were stored in 300 μl RNA-Protect Cell Reagent (Qiagen). Total RNA was prepared from the cell pellet using the Purelink RNA mini kit (Invitrogen) and homogenizer spin columns according to the manufacturer's directions. Total RNA concentrations, A260/A280 ratios, and RIN values were determined using an Agilent 2100 Bioanalyzer (Agilent Technologies). Equal amounts of total RNA from each sample were used for quantitative polymerase chain reaction (qPCR) analysis. First, the samples were subjected to genomic DNA elimination and first strand cDNA synthesis using a commercial kit (RT^2 First Strand Kit; SA Biosciences) to generate the cDNA templates for PCR amplification. Quality control was performed using the SA Biosciences QC qRT-PCR array (SA Biosciences) to test for any inhibition of cDNA synthesis, or presence of genomic DNA contamination. Gene expression assays were performed using sets of premade mouse primer pairs (SA Biosciences; see Supplementary Tables for primer catalog numbers). qPCR was performed using a Stratagene MX3000P Detection system or ABI7500, and RT^2 qPCR SYBR green PCR Master Mix (SA Biosciences) according to the manufacturer's recommended protocol. Each sample was analyzed in triplicate, normalized using the housekeeping genes *Hrpt1*, *Gapdh*, and *GusB*, and relative gene expression was calculated using the comparative C_t method [1].

Immunocytochemistry and immunohistochemistry

For immunostaining of cryosections, samples were fixed with 2% formalin (2 min) and washed (Tris buffered saline [TBS]) 3 times before a 20 min protein block (Dako), and exposure to the primary antibodies (16 h, 4°C). Detection of the primary antibodies was achieved using donkey anti-mouse Alexa Fluor 488 at 1:200 (30 min at 37°C).

For immunocytochemistry in cultured cells, subconfluent (80%–90%) cells were fixed in methanol (−20°C) and stained without antigen retrieval by incubation with primary rabbit polyclonal anti-mouse antibodies (1:100, 1 h, room temperature [RT]) (Abcam) or monoclonal antibodies (Santa Cruz) against laminin (Ab11575, polyclonal), collagen 1 (Ab34710, polyclonal), collagen IV (Clone 10B7), fibronectin (Clone IST-9), vimentin (Clone RV202), and alpha smooth muscle actin (Ab5694, polyclonal) or respective isotype control antibodies. For detection, species-specific peroxidase-conjugated secondary antibodies (Vector Laboratories) or Alexa 595-conjugated donkey anti-mouse IgG were incubated with samples (37°C, 30 min).

Flow cytometry reagents

The following antibodies (clones) used to characterize L-MSCs and BM-MSCs were obtained from eBiosciences unless otherwise indicated: CD31/PECAM (MEC13.3; BD), CD45.2 (104), CD14 (Sa2-8), CD44 (IM7, BD), CD73/5′-nucleosidase (TY/11.8), CD90.2/Thy-1 (13H12, BD), CD105/endoglin (MJ7/18), CD 106/VCAM-1 (429), CD166/ALCAM (ALC48), integrins alpha (Itg α)2 (HMalpha2, BD), Itg α3 (FAB2787A; R&D Systems), Itg α4 (R1-2), Itg α5 (HMalpha5-1, BD), Itg α6 (GoH3), Itg α8 (BAF4076, R&D) or Itg αV (RMV-7), Itg β1 (HMb.1), Itg β3 (2C9.G3), Itg β5 (ALULA, Dean Sheppard, UCSF), Itg β6 (Amha, Dean Sheppard, UCSF), CD36 (72–1), Sca-1 (D7), flk-1 (Avas2alpha-1, BD), CD34 (MEK14.7, Caltag), CD117/c-kit (2B8, BD), CD47 (miap301), CD56/NCAM (MEM188; Abcam), PDGFRα (APA5), PDGFRβ (APB5), CD54/ICAM-1 (YN1/1.7.4), ICAM-2/CD102 (3C4), CD146/MCAM (P1H12, Abcam), NGFR/p75/CD271 (H-137, Santa Cruz, Santa Cruz, CA), or CD133/Prominin (13A4), P-selectin/CD62P (K02.3), PSGL1/CD162 (2PH1, BD), E-selectin/CD62E (10E9.6, BD), CD24 (M1/69), Itg β2/CD18 (M18/2), and CD11a (M17/4), CD11b (M1/70), CD11c (N418), and F4/80 (BM8).

Reference

1. Pfaffl MW. (2001). A new mathematical model for relative quantification in real-time RT-PCR. Nucleic Acids Res 29:e45.

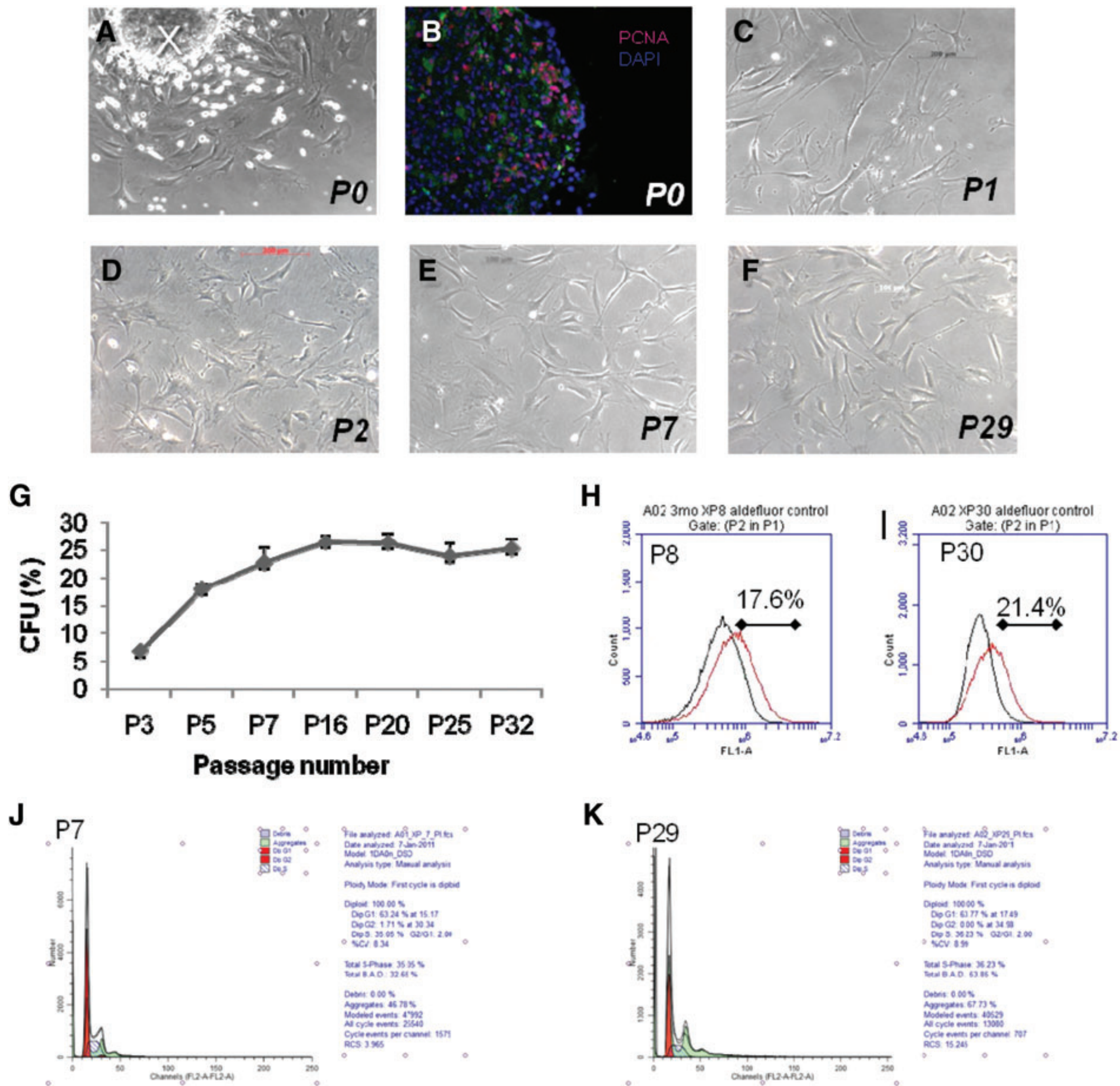

SUPPLEMENTARY FIG. S1. Morphology, clonogenicity, aldehyde dehydrogenase expression, and ploidy of early versus late passage L-MSCs. **(A)** Explants ("X") yielded primarily fibroblastic cells when grown on plastic in minimal media (alpha MEM, 15% FBS), 50×; initial growth is designated as passage 0 (P0), day 7. **(B)** Proliferative ($PCNA^{pos}$) cells on day 7 are seen in the explants tissue migrating toward the edge, 50×; the exact in vivo location could not be established by this technique due to atelectasis of tissues. **(C)** Outgrowth cells show heterogeneity in size and morphology (crescent, spindle, and stellate-shaped cells) in P1 and P2 **(C, D)**, but from P7 to P29 **(E, F)** crescent-shaped cells predominated. **(G)** Colony-forming units (% of 2,000 cells/plate, $n=3$ plates/experiment) from P3 to P32 show a significant increase and plateau from P3 to P7; P7 cells were used for in vitro and transplantation assays due to greater consistency in CFU (%) and morphology. **(H, I)** Aldehyde dehydrogenase (ALDH; Aldefluor, Stem Cell Technologies)-positive cells at P7 versus P30, which shown similar profiles. Note that the percentage of $ALDH^{pos}$ L-MSCs is similar to CFU (%). **(J, K)** Analysis of cell cycle kinetics showing that ~35% of P7 or P29 cells were in S phase and ~100% of P7 or P29 cells were diploid; cell cycle data were acquired on Accuri C6 (100,000 events) and analyzed using commercial software (ModFit). FBS, fetal bovine serum; L-MSCs, lung-derived mesenchymal stromal cells; FBS, fetal bovine serum; CFU, colony-forming units; MEM, minimum essential media.

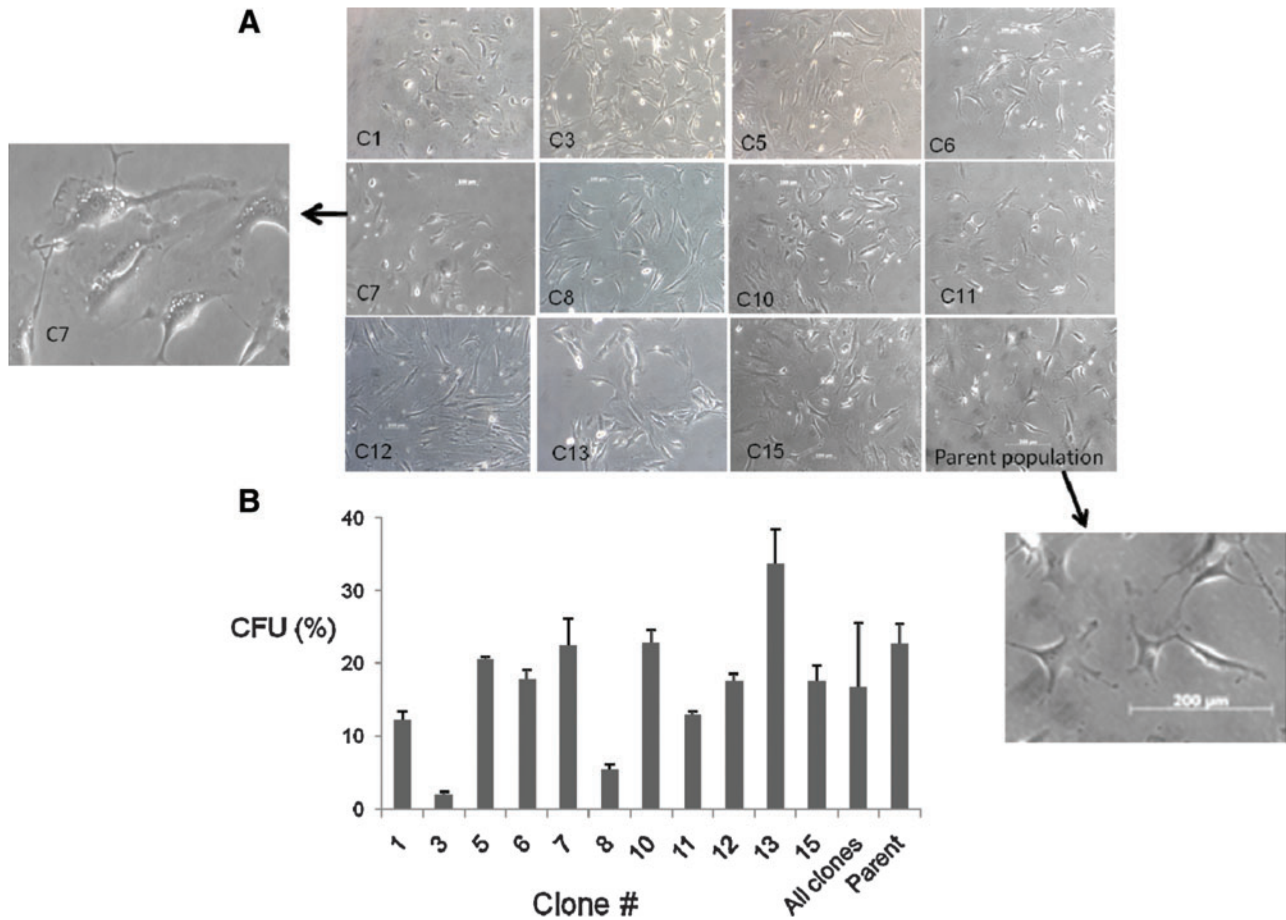

SUPPLEMENTARY FIG. S2. Morphologic appearance and colony-forming efficiency of clones derived from L-MSCs parent population (passage 4) by limited dilution. **(A)** Panel of phase-contrast photomicrophages (100×) showing subtle variation in distribution of morphologies (at passage 7) of clones (identified in *lower left corner*). Variation in morphology from crescent-shaped (eg, C3, C6) to more spindle-shaped (eg, C5, C12) cells with rare myofibroblastic stellate cells are noted in clones cultured identically; one clone (C7) exhibited lipid vesicles in their cytoplasm (also see enlarged photomicrograph to *left of panel*). The parent population typically contained a mixture of morphologies as did clonal populations after serial passage, suggesting that variation in morphology is an intrinsic property of each subculture. **(B)** Colony-forming efficiency varied considerably between clones (∼3%–35%); the mean ± standard deviation of all clonal CFUs versus the parent population ($n=3$ replicates) were very similar; therefore, the parent L-MSCs contain subsets of L-MSCs with marked differences in CFU.

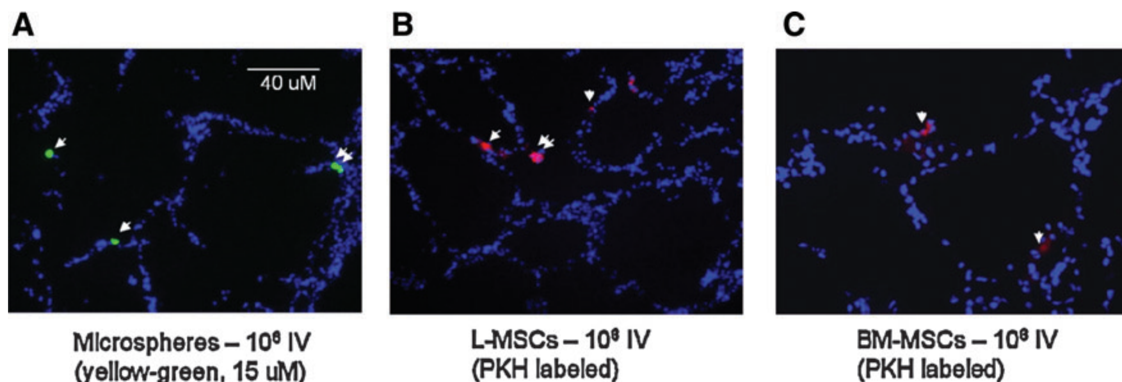

SUPPLEMENTARY FIG. S3. Low magnification (100×) photomicrographs of lung cryosections from mice with chronic emphysema that were euthanized immediately after injection with 1 million **(A)** 15 μM microspheres (yellow-green fluorochrome, Invitrogen), or PKH26-labeled **(B)** L-MSCs, or **(C)** BM-MSCs. Cells were found to distribute randomly, independent of the extent of elastase injury. In cryosections (10 μM) they were found as singlets (*single arrows*) or small clusters (2–3 cells, *double arrows*) at low density (1–2/hpf), similar to the distribution of microspheres. hpf, high powered field.

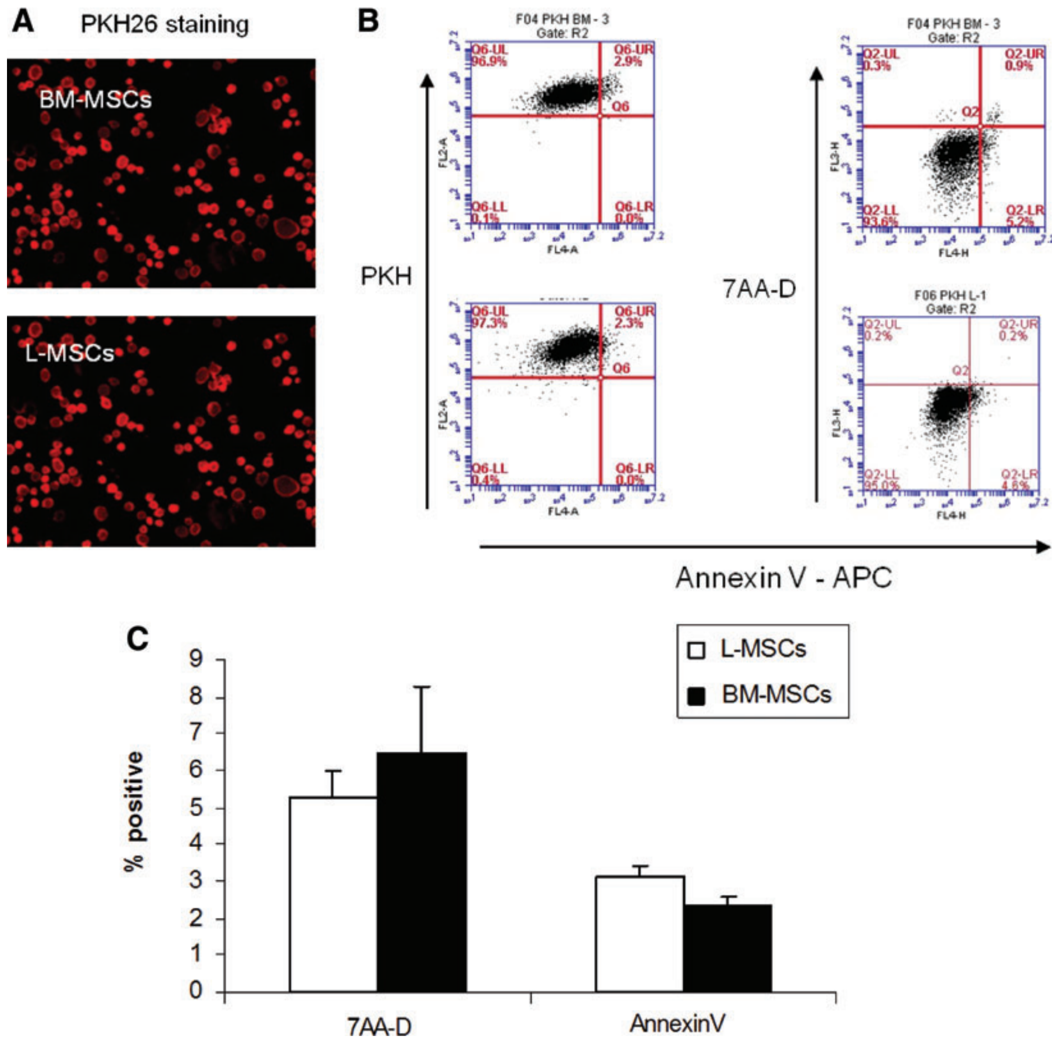

SUPPLEMENTARY FIG. S4. Effect of PKH cell-labeling procedure on survival and apoptosis in L-MSCs versus BM-MSCs. Cells were labeled (5 min) with PKH26 (Sigma) according to the manufacturer's recommendations. The intensity of staining was equivalent for cell lines **(A, B)**. There was no effect of PKH26 labeling on the incidence of apoptosis (Annexin V^{pos}, Annexin V staining kit, eBioscience) or cell death (7AA-D^{pos}) in L-MSCs and BM-MSCs **(C)**. APC, allophycocyanin.

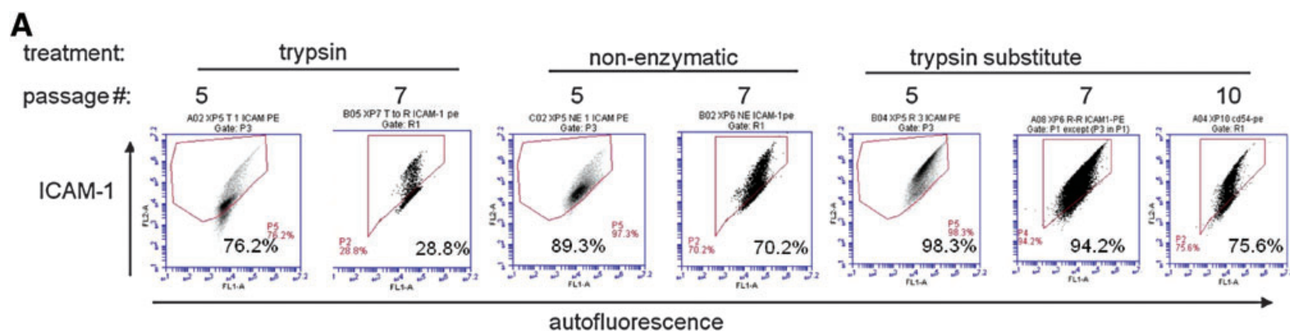

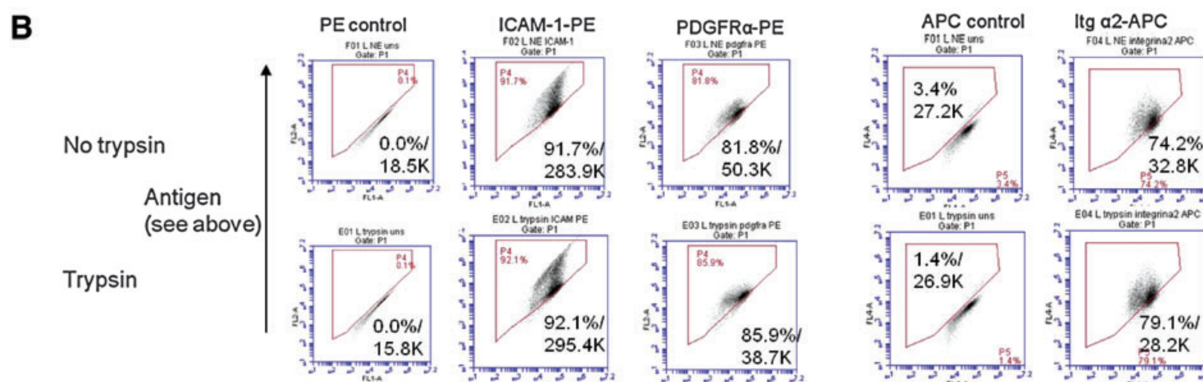

SUPPLEMENTARY FIG. S5. Effect of trypsin harvest of L-MSCs on ICAM-1 expression and detection. **(A)** Trypsin was used at each passage (1–7) and caused a marked diminution of ICAM-1 expression when compared with the effects of passaging with either a nonenzymatic reagent (Enzyme-free cell dissociation; Millipore) or nonanimal–nonhuman origin trypsin substitute (TrypLE Express; Invitrogen), the latter of which maintained high (>75% positive) ICAM-1 expression to at least passage 10. **(B)** Detection of ICAM-1, PDGFRα, and Itg α2 was not affected by harvesting cells with trypsin/ethylenediaminetetraacetic acid. ICAM-1, intercellular adhesion molecule 1; PDGFRα, platelet derived growth factor.

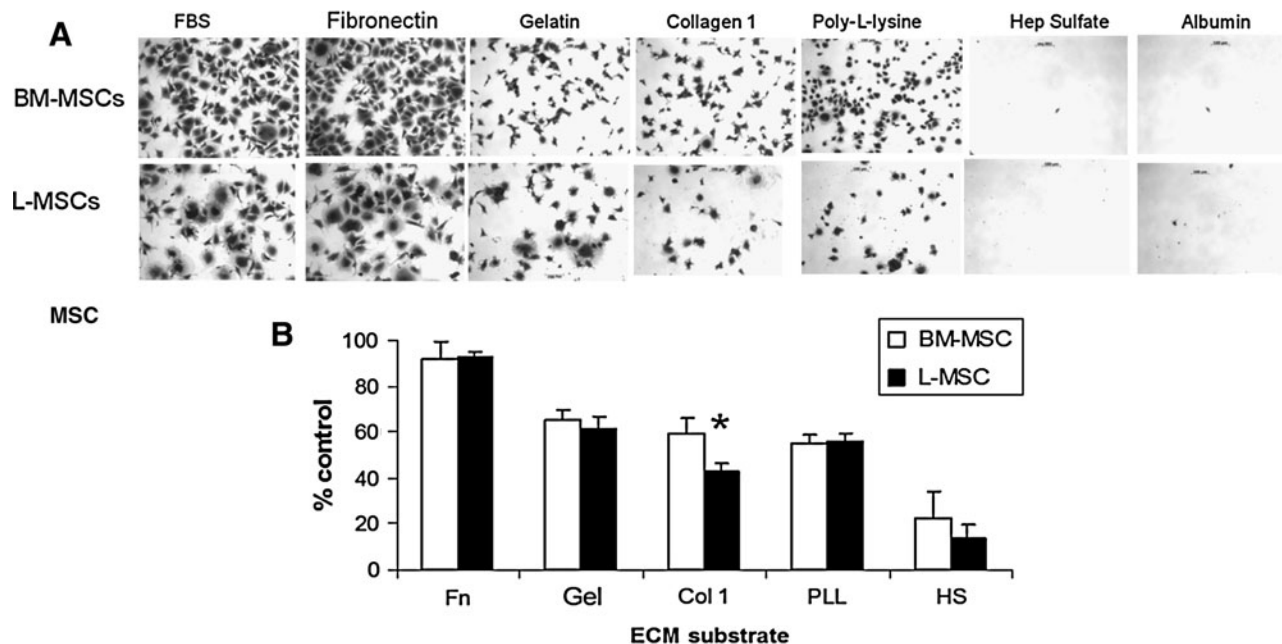

SUPPLEMENTARY FIG. S6. Comparison between L-MSCs and BM-MSCs for extracellular matrix substrate binding on precoated tissue culture plates (20 μg/mL, 1 h, 23°C). **(A, B)** These binding assays revealed that L-MSCs bound collagen 1 less avidly ($*P<0.05$) than BM-MSCs, but adherence to other common matrix proteins was not statistically different. Fn, fibrinogen; Gel, gelatin; Col 1, collagen 1; PLL, poly-L-lysine; HS, heparin sulfate; FBS and albumin are shown as positive and negative controls, respectively **(A)**.

Supplementary Table S1. Differentiation Assays Were Performed on Lung-Derived Mesenchymal Stromal Cells Cultured as Described in the Methods

Gene symbol	*Gene name*	*Primer catalog number*	*Fold change*	P
Alveolar epithelial type I cell				
Aqp5	Aquaporin 5	PPM29204A	3.05	< 0.01
Clara cell				
Scgb1A1	Clara cell secretory protein	PPM05626B	5.06	< 0.005
Alveolar epithelial type II cell				
Sftpc	Pro-surfactant protein C	PPM26536A	0.06	N/S
Ttf-1	Transcription termination factor, RNA polymerase I	PP35192AM	1.31	N/S
Endothelial cell				
CD31	Platelet endothelial cell adhesion molecule	PPM03802C	1.02	N/S
Cdh5	CD144/VE Cadherin	PPM03797B	1.43	N/S
Flk-1	Kinase insert domain protein receptor	PPM03057A	−2.37	< 0.01
Vwf	von Willebrand factor	PPM05310E	2.50	< 0.005
Smooth muscle cell				
Des	Desmin	PPM25379A	3.75 3.75	< 0.0001
MyoD1	Myogenic differentiation 1	PPM04481A	7.6	< 0.005
Acta2	α smooth muscle actin	PPM04483A	4.11	< 0.0001
Adipocyte				
Lpl	Lipoprotein lipase	PPM04353E	109.4	< 0.0001
Fabp4	Fatty acid binding protein	PPM04517A	1.14	N/S
Pparγ	Peroxisome proliferator activated receptor gamma	PPM05108B	26.6	< 0.0001

Transcription was measured using quantitative real-time PCR. *P* values represent analysis of mean C_t values using independent *t*-tests and Bonferroni adjustment of *P* value (< 0.01 considered significant). PCR, polymerase chain reaction.

Supplementary Table S2. Effect of Transforming Growth Factor Beta 1 on Lung-Derived Mesenchymal Stromal Cells Expression of Genes Encoding Proteins Related to Lung-Derived Mesenchymal Stromal Cells Differentiation to Myofibroblasts, Fibroblast Activation, Survival, and Senescence

Gene symbol	*Gene name*	*Primercatalog number*	*Fold change*	P
Acta2	α smooth muscle actin	PPM04483A	1.8	0.025
Col1A1	Collagen 1	PMM03845F	2.8	0.001
Fn1	Fibronectin	PPM03786A	2.2	0.000
Lox	Lysyl-oxidase	PPM04652A	2.5	0.000
Mmp9	Matrix metalloproteiase-9	PPM03661B	50.4	0.000
Tnc	Tenascin	PPM03804E	2.0	0.000
Tnrsf12A	TweakR	PPM27298A	1.9	0.000
Dpp4	Dipeptidyl-peptidase 4/CD26	PPM05502A	−3.0	0.012
Fap α	Fibroblast-activating protein	PPM28904A	1.0	0.879
S100A4	Fibroblast specific protein 1	PPM03811A	−2.1	0.001
Birc5	Baculoviral IAP repeat containing 5	PPM03431B	−2.0	0.001
Mdk	Midkine	PPM03800B	−1.3	0.033
Cdkn1a	Cyclin dependent kinase 1a/p21	PPM02901A	1.5	0.029
Tp53	Tumor protein 53	PPM02931B	1.4	0.000

Passage 7 L-MSCs previously incubated in serum-free media (6 h) were exposed to human recombinant TGFβ1 (10 ng/mL, R&D Systems) or PBS vehicle (48 h). Samples were run in triplicate by quantitative real-time PCR using commercial primers (SA Biosciences) as shown; fold differences (TGFβ1/control) are reported in association with *P* value (< 0.05 considered significant); the average mRNA expression of housekeeping genes *Hrtp1*, *GusB*, *GAPDH* was used to normalize data. TGFβ1-induced genes associated with myofibroblastic phenotype, but not activation. Survival genes were significantly suppressed and senescence associated genes activated, consistent with terminal differentiation by TGFβ1. L-MSCs, lung-derived mesenchymal stromal cells; FBS, fetal bovine serum; PBS, phosphate-buffered saline; GAPDH, glyceraldehyde 3-phosphate dehydrogenase; TGFβ1, transforming growth factor beta 1.

Supplementary Table S3. Gene Expression Arrays Comparing mRNA Expression by Quantitative Real-Time Polymerase Chain Reaction in Lung-Derived Mesenchymal Stromal Cells Versus Bone Marrow-Derived Mesenchymal Stromal Cells (P7), Employing 3 Commercial Arrays That Were Focused on Extracellular Matrix Genes (PAMM-13, SA Biosciences), Growth Factors (PAMM-043, SA Biosciences), or Chemokine/Cytokine (PAMM-022, SA Biosciences) Signaling

ECM array		
Gene	*Fold change*	*P value*
	L-MSC over-express	
Adamts1	4.065	0.01291
Adamts2	2.561	0.0033
Ctnna1	1.610	0.02682
Ctnnb1	1.761	0.01117
Col3a1	1.502	0.04543
Emilin1	3.227	0.00336
Fbln1	13.674	7.8E-05
Icam1	69.391	0.00086
Itga2	3.403	0.0025
Itgb2	3.466	0.01212
Itgb3	2.292	0.00652
Lama1	3.927	0.03236
Lama3	2.670	0.0218
Lamb2	2.080	0.00268
Lamc1	1.828	0.00462
Mmp13	9.647	0.00423
Mmp14	2.179	0.01661
Mmp3	80.263	0.00125
Postn	8.301	0.00103
Selp	49.522	0.00238
Sgce	2.633	0.00305
Thbs2	4.490	0.00585
Thbs3	3.515	0.01858
Vcam1	1.606	0.04023
Gene	*Fold change*	P value
	BM-MSC over-express	
Col2a1	4.056	0.02636
Col6a1	1.434	0.04734
Ctgf	3.991	0.0007
Ecm1	1.741	0.00679
Itga3	9.084	0.00502
Itga5	3.597	0.00015
Ncam1	1.613	0.00831
Mmp2	2.701	0.00102
Spp1	34.776	0.00081
Thbs1	1.566	0.01626
Tnc	8.938	0.01582

Growth factor array		
Gene	*Fold change*	*P value*
	L-MSC over-express	
Artn	3.067	0.035058
Bdnf	2.139	0.017743
Bmp4	2.682	0.026182
Bmp6	4.065	0.017484
Csf1	1.505	0.019377
Csf2	8.714	0.006229
Cxcl1	23.807	0.001595
Cxcl12	6.997	0.000108
Ereg	3.110	0.003191
Fgf11	1.414	0.010363
Fgf18	20.726	0.000177
Figf	26.416	0.000307
Gdnf	10.267	0.000153
Hgf	15.313	0.000035
Igf2	86.223	0.000041
Il11	6.981	0.012981
Il18	2.189	0.016084
Il6	24.196	0.000002
Kitl	3.418	0.000968
Lefty1	17.268	0.000137
Lif	1.505	0.000768
Ngf	2.119	0.001635
Pgf	5.762	0.000001
Rabep1	2.129	0.003205
Vegfa	1.888	0.005948
Vegfb	3.450	0.008254
Vegfc	1.537	0.019247
	BM-MSC over-express	
Igf1	2.139	0.013488
Inhba	4.327	0.011562
Inhbb	13.801	0.010316
S100a6	2.567	0.000105
Spp1	44.017	0.000372
Tgfb2	4.209	0.000038
Tgfb3	1.807	0.001317

Chemokine/Cytokine array		
Gene	*Fold change*	*P value*
	L-MSC over-express	
Bmp6	4.317	0.020665
Ccl2	19.338	0.011608
Ccl5	19.027	0.013155
Ccl7	20.112	0.01486
Ccl9	4.357	0.016915
Ccll2	4.779	0.017255
Cmtm3	2.802	0.02651
Cxcr7	62.683	0.013626
Csf2	16.074	0.011197
Cxcl1	29.651	0.002251
Cxcl10	62.394	0.011909
Cxcl11	3.490	0.039062
Cxcl12	4.681	0.028183
Cxcl2	36.085	0.000276
Cxcl9	1.968	0.005476
Il18	2.457	0.002076
Lif	1.737	0.046443
Myd88	6.262	0.000073
Nfkb1	1.786	0.002087
Slit2	3.395	0.000017
Tlr4	1.819	0.000518
Tnfrsf1a	1.853	0.001733
	BM-MSC over-express	
Ccl17	2.770	0.043895
Cx3cl1	3.613	0.000466
Ppbp	3.531	0.001449
Inhbb	10.459	0.000126
Mmp2	3.024	0.000015

Primer sequences are available at the SA Biosciences Web site: (www.sabiosciences.com/ArrayList.php?pline=PCRArray). Samples were performed in triplicate. Shown are fold changes ("*Fold change*," L-MSCs/BM-MSCs) for each gene. The average mRNA expression of housekeeping genes *GusB* and *GADPH* was used to normalize these data. Genes selected for further analysis of paracrine signals in vivo are shown in boxes; $P < 0.05$ was considered significant. BM-MSCs, bone marrow-derived mesenchymal stromal cells; ECM, extracellular matrix.

Supplementary Table S4. List of Genes and Primers Used in Quantitative Real-Time Polymerase Chain Reaction Analysis of mRNA Expression in Whole Lung Tissues Transplantated with Lung-Derived Mesenchymal Stromal Cells, Bone Marrow-Derived Mesenchymal Stromal Cells, or Phosphate-Buffered Saline In Vivo

Gene symbol	*Gene name*	*Primercatalog number*
Ccl2	Chemokine C-C motif ligand 2	PPM03151F
Ccl5	Chemokine C-C motif ligand 5	PPM02960E
Cxcl2	Chemokine CXC motif ligand 2	PPM02969E9E
Cxcl10	Chemokine CXC motif ligand 10	PPM02978D
Cxcl12	Chemokine CXC motif ligand 12	PPM02965E
Cxcr7	Chemokine CXC receptor type 7	PPM03179A
Fgf18	Fibroblast growth factor 18	PPM03046B
Hgf	Hepatocyte growth factor	PPM02953C
Igf2	Insulin-like growth factor 2	PPM03655A
S100A4	Fibroblast specific protein 1	PPM03811A
IL-6	Interleukin 6	PPM03015A
IL-11	Interleukin 11	PPM03018E
Spp1	Secreted phosphoprotein 1	PPM03648C

Results are summarized in Fig. 7A.